Combined experimental and theoretical investigation of electronic properties of nitrides

N. N. Jandow[1], *M. M. Khan*[2,*]

[1]Department of Physics, Faculty of Education, Al-Mustansiriyah University, Baghdad, Iraq
[2]Chemical Sciences, Faculty of Science, Universiti Brunei Darussalam, Jalan Tungku Link, Gadong, BE 1410, Brunei Darussalam
*) Email: khanmm@ubd.edu.bn

Received 1/2/2022, *Accepted,* 16/9/2022, *Published* 15/10/2022

A comprehensive study of the electronic structure of group-III nitrides (AlN, GaN, InN, and BN) crystallizing in the wurtzite, zinc-blende, and graphitelike hexagonal (BN) structures is presented. A large set of the x-ray emission and absorption spectra was collected at the several synchrotron radiation facilities at installations offering the highest possible energy resolution. By taking advantage of the linear polarization of the synchrotron radiation and making careful crystallographic orientation of the samples, the bonds along *c* axis (*rr*) and ''in plane'' (*u*) in the wurtzite structure could be separately examined. Particularly for AlN we found pronounced anisotropy of the studied bonds. The experimental spectra are compared directly with *ab initio* calculations of the partial density of states projected on the cation and anion atomic sites. For the GaN, AlN, and InN the agreement between structures observed in the calculated density of states (DOS) and structures observed in the experimental spectra is very good. In the case of hexagonal BN we have found an important influence of insufficient core screening in the x-ray spectra that influences the DOS distribution. The ionicityof the considered nitrides is also discussed.

Keywords: Electronic; BN; Band structure.

1. INTRODUCTION

The group-III nitrides (GaN, AlN, InN, and BN) are wide- gap refractory semiconductors with applications as basic materials in optoelectronic devices operating in the visible/ ultraviolet spectral range as well as in high-temperature and high-power microelectronic devices [1,2]. However, the under- standing of the basic physical properties leading to applications is still not satisfactory. One of the reasons consists of insufficient knowledge of the electronic band structure of the considered semiconductors being somewhat ‘‘untypical’’ comparing to the ‘classic’’ III-V materials. Apart from BN the nitrides crystallize in the thermodynamically stable wurtzite structure and in the metastable sphalerite (zinc- blende) structure (cubic). BN has hexagonal and cubic phases similar to the graphite and diamond phases of carbon. Recently, several other metastable structures have been identified (rhombohedral, wurtzite, simple cubic, and turbostratic) [3], and also a fullerenelike structure has been synthesized and characterized [4]. The coordination number is the same, in all structures examined here. There are, nevertheless, some differences in physical properties of these nitride phases, where the most important physical parameters of nitrides are summarized. In all mate- rials and structures nitrogen as an anion leads to the formation of very short, strong bonds. Comparing to other III-V semiconductors, we find the bond lengths in nitrides approximately 20% shorter (e.g., 1.95 Å for wurtzite GaN in comparison with 2.7 Å in GaAs) and the ionicity roughly two times higher [5-7].

Several theoretical studies of III-V nitrides have been published but surprisingly, relatively few experimental studies of the band structure have been carried out [8-12] except for BN. Only recently some x-ray studies concerning mainly GaN have been published [13-16]. The shape of the x-ray spectra is a fingerprint of the particular chemical bond and makes it possible to identify the chemical nature of the bond formed by selected kind of atoms in different com- pounds. Photon absorption and emission involves an optical transition between electronic states of the atom in the sample. This allows the interpretation of the experimental spectra in terms of the density of the occupied states (valence band) for emission and density of unoccupied states (conduction band) for absorption spectra. The electron transition is governed by dipole selection rule and hence the investigated electronic states are also ‘‘orbital resolved.’’ The linear polarization of the synchrotron radiation allows a separation of crystallographic-direction-dependent contributions from various constituents to the band states and thus a description of the anisotropy of chemical bonding. In the present paper a systematic experimental and theoretical study of atom- and orbital-projected partial density of states (DOS) for the group-III nitrides is reported. We com- pare the energy distribution of electronic states in valence and conduction bands as calculated by means of the linear muffin-tin orbital (LMTO) method with x-ray emission and absorption spectra. We do not attempt to calculate the DOS with the broadening functions to account for the lifetime of the involved core levels and spectrometer resolving functions to mimic exactly the relative intensity between peaks observed in spectra. Instead, the direct comparison with the appropriate ‘‘raw’’ DOS is presented to indicate the extent to which we can get direct information about allowed electron states by consideration the positions of the maxima and minima of the intensity in spectra. The influence of the core level width and spectrometer broadening function on the spectral structures is also discussed.

The good agreement between structures observed in spectra and structures in the calculated DOS allows for consistent analysis of the results. We compare the amounts of bonding and antibonding states near the band edges for different choices of cations and crystal structures. Since the device applications are based mainly on wurtzite-type nitrides, particular attention is paid to this phase. In particular, we examine for wurtzite structure the level of anisotropy

in the formed chemical bonds along the *c* axis (*rr* bond) and ''in plane,'' i.e., slightly inclined with respect to the *c* plane (*u* bonds). These two kinds of bonds, *rr* and *u*, can be connected directly with *b* and *d* bond lengths, respectively. Theirvalues as obtained by x-ray diffraction measurements.

Finally, we examine the amount of electronic states avail- able for optical transition as a function of crystal structure, crystallographic direction, and the presence of *d* cation semicore states. The role of the cation semicore *d* states in the determination of different properties of group-III nitrides hasbeen discussed by several authors.[8] In this context the hy- bridization between *d* and *p* states for different cations and nitrogen is investigated. The *d-p* interaction can affect the valence-band edge and may influence magnitude of the fundamental gap. It has been suggested that the cation- 4*d* –anion-*p* hybridization is stronger in AlN than in GaN.

2. EXPERIMENT

The x-ray absorption and emission measurements for lines with energy up to 600 eV were performed at the Lawrence Berkeley National Laboratory (LBNL) Advanced Light Source (ALS) at the beam lines 6.3.2 and 8.0, respectively.[18] In the case of x-ray absorption the total pho- tocurrent measurement technique was applied for recording of the spectra. The energy resolution !J*E* for the 1200 line/mm grating employed for nitrogen *K* edge (with a 50 μm exit slit) was close to 0.16 eV. The $M_{2,3}$ edge of Ga, $L_{2,3}$edge of Al, and *K* edges of *B*, were measured using a 300 line/mm grating with a 50 μm exit slit, which results inresolution 0.2 eV, 0.04 eV, and 0.03 eV, respectively. Measurements of $L_{2,3}$ edges of Ga and *K* edges of Al were car- ried out at the SA32 station of the SuperAcoring, LURE.The $L_{2,3}$ edges of Ga were measured using a Be(1010) monochromator, which provides an energy resolution of !J*E*~0.6 eV, and the *K* edges of Al were measured with a quartz (1010) monochromator with a resolution of !J*E*~0.6 eV. The Ga *K*-edge data were recorded using a Si (111) monochromator at the D-21 station, DCI ring, LURE and with higher resolution using the four crystalline Si monochromators in HASYLAB, station A1. At this station also the In *L*-edge spectra were measured.

The spectra of wurtzite structure samples were recorded atdifferent angles between the single crystalline sample surface (its *c* plane) and the polarization vector of synchrotron radiation. At normal incidence the polarization vector **e** was par- allel to the sample surface, and electrons were excited in the direction of the *c* plane probing three *u* bonds out of the four forming a tetrahedral coordination. At grazing incidence, the polarization vector **e** formed a small angle with the *c* axis (which is normal to the sample surface). Therefore, the states localized along the *c* axis (single *rr* bond) should predominate the spectra. In the case of large anisotropy (AlN) the spectra were also measured at an angle 46° to the surface where both bonds should be probed. For epitaxial layers the photocurrent was measured from an isolated sample. In the hard x-ray region, the intensity at I_0 was monitored by an ionization chamber with proper pressure and mixture of gases in the soft energy region by the photocurrent generated at the focusing mirror. Additional transmission measurements were performed on GaN and InN powders to test the influence of surface oxides on the absorption. The spectra registered in transmission and at the angle of 46° were identical. Therefore, the influence of the surface contaminationon the spectra from layers was negligible.

High-resolution x-ray emission spectra were recorded athe ALS station 8.0 on the 5.0 cm period undulator beamline with a spherical grating monochromator operating between 70 eV and 1200 eV.[19] The *K*-emission spectra of N were measured using the 1000 line/mm, 10 m

radius grating. At the 400 eV energy the resolution of the spectrometer was approximately 0.8 eV and at the 200 eV about 0.5 eV. The energy of the excitation radiation was set high above resonant excitation. The samples of polycrystalline, hexagonal, and cubic BN and wurtzite GaN and InN were commercially available powders (with particles size smaller than 20 μm). For these samples we were not able to measure polarization resolved spectra. The wurtzite GaN and InN films were grown by molecular beam epitaxy (MBE) on sapphire substrate. The nucleation and growth of the wurtzite AlN and cubic GaN and InN films were performed in the MBE system on singular (001) n+Sn-doped GaAs substrates. The thicknesses of the epitaxial layers used in our measurements were between 0.5 and 1 μm. Transmission electron microscopy (TEM) cross-section and x-ray diffraction studies have clearly shown formation of single wurtzite or cubic phases.

The band structure and DOS for the all group-III nitrides in wurtzite and zinc-blende structures are calculated by means of the LMTO method in its scalar relativistic form, in conjunction with the local density approximation (LDA) to the density functional theory. Here we apply the simplest version of the LMTO method, the atomic-sphere approximation (ASA) but with the ''combined correction'' terms incorporated. The ASA version applies spherically symmetrized charge distributions and potentials in atomic spheres, i.e., space filling (and thus slightly overlapping) spheres. Consequently, calculations for the semiconductors must include so-called ''empty spheres'' located in the interstitial positions, i.e., atomic spheres without ''nuclear'' charge. Each unit cell in the cubic (zinc-blende) structure contains two real atoms (cation and anion) and two empty spheres. In the wurtzite structure we have eight atoms in the unit cell (four ''real'' and four ''empty'').

In the calculations presented here we have used the ''standard'' basis set, which includes partial waves of s, p, and d character on each atomic and interstitial site to give a total of 36 LMTO orbitals per cubic unit cell. The ''semicore'' shal- lowed d states in GaN and InN are treated as fully relaxed band states. This is especially important for GaN, as it was already shown.[8] Energy eigenvalues and wave functions were obtained at 95 (140) **k** points in the irreducible part of the Brillouin zone. The densities of states, normalized to the unit cell, were calculated by means of the tetrahedron technique. The calculations for wurtzite structure were performed under the assumption that the crystal structure was ''ideal,'' meaning that the c/a ratio was taken as equal to 1.633 and the internal bond-length parameter u was 3/8. Experimental c/a values are 1.627, 1.600, and 1.612 for GaN, AlN and InN, respectively.[23] X-ray diffraction measurements have shown that u=0.377 for GaN and 0.3821 for AlN. The calculations for hexagonal BN were performed by a slightly different method, the full-potential version[25] of the LMTO scheme, where the full non-spherical shapes of potentials and charge distributions are taken into account.

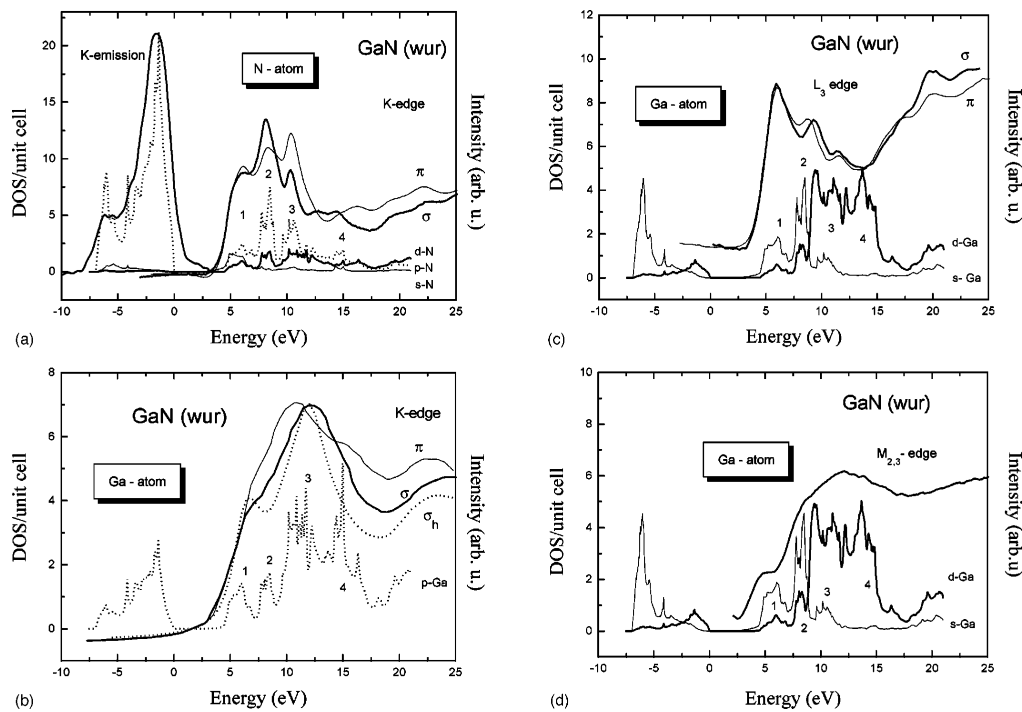

Figure 1 The PDOS (*s* thin line; *p*, dotted line; *d*, thick line) as calculated for the wurtzite structure of GaN. (a) Projected on the N atom and compared with N *K* emission and absorption spectra for *rr* and *u* polarization geometry. (b) Projected on the Ga atom: *p* PDOS compared with Ga *K* absorption spectra measured for *rr* and *u* polarization geometry. Additionally, the high-resolution *u* spectrum is shown (dotted line). (c) Projected on the Ga atom: *s* and *d* PDOS compared with Ga L_3 absorption spectra measured for *rr* and *u* polarization geometry. (d) Projected on the Ga atom: *s* and *d* PDOS compared with the Ga $M_{2,3}$ absorption spectrum.

3. RESULTS AND DISCUSSION

Figures 1 through 8 show the partial DOS (PDOS), as obtained by the LMTO method and projected onto the atomic sites, together with the experimental x-ray emission and absorption spectra, for wurtzite and cubic GaN, AlN, InN, and for hexagonal and cubic BN. Linearly polarized synchrotron radiation irradiating well-oriented samples of wurtzite GaN, AlN, and InN allowed us to precisely examine the anisotropy of the bonds formed in this structure. The reference energies of the experimental spectra were adjusted to give the best overall agreement of the characteristic spectral features of the theoretical DOS functions. The energy zero corresponds to the valence-band (VB) edge. On the left vertical axis the calculated total or partial (s, p, d) DOS per unit cell at the chosen atom is indicated, which allows us to compare the absolute number of the available states. Note that the number of atoms in the wurtzite unit cell is two times larger. Therefore, for direct comparison the number of states in the cubic structure should be multiplied by a factor. On the right vertical axis, the intensity of experimentally measured spectra in arbitrary units is shown. The spectra measured at different angles were normalized to the equal intensities before the onset of edge and far above the conduction band (CB) edge where no polarization dependence is expected.

The GaN absorption spectra have been already discussed,[13–15] but importantly, with the spectra recorded for different polarization we were able differentiate contributions of *u* and *rr* bonds to the particular structures in the density of states. Figure 1(a) contains the

experimental emission and absorption spectra at the *K* edge of nitrogen, which correspond to contribution of *p* states of N to the valence and conduction bands, respectively. Additionally, calculated PDOS representing contributions of *s*, *p*, and *d* states of N are shown. The states are localized in easily seen sub-bands with energy positions that agree with the maxima in observed emission and absorption spectra. The crystal field splits the valence states into two subbands and the conduction states, in the considered energy range, into four separate sub-bands. As one can see the *p* states dominate over all other states. Note, however, that the conduction-band edge has also a significant contribution of nitrogen *s* states. A similarity of the measured spectrum with the calculated *p* DOS supports the dominant character of *p* states in the valence and conduction bands. Considering the anisotropy of *p* states as seen by contributions from *rr* and *u* bond states (measured by different polarizations of synchrotron beem) some moderate differences in peak intensities and in position of peak number 4 can be noticed.

For the Ga atom the absorption spectra have been measured only [Figs. 1(b,c,d)]. In Fig. 1(b) *K*-edge absorption spectra (*rr*, *u*, and high-resolution *u*) in comparison with calculated *p* PDOS are shown. As in the case of nitrogen [Fig. 1(a)], one can notice the existence of four subbands in the calculated PDOS corresponding to the main features of the measured absorption spectra. However, the anisotropy of states distribution is more pronounced in comparison with nitrogen *rr* bonds. The maximum of *rr* Ga bond states is now 2 eV closer to the CB edge than the maximum of *u* bond states. Also, the second and fourth maxima consist of predominately *rr* bond states. Consequently, in the *c* direction for the indicated energies there are much more available states than ‘‘in plane.’’ The observed anisotropy can influence the optical and transport properties in plane and in the *c* direction.

In Figs. 1(c) and 1(d) the L_3 and $M_{2,3}$ absorption spectra of Ga are shown together with the calculated PDOS of *s* and *d* symmetry. We observe in the case of the L_3 edge three well-resolved peaks that correspond preferentially to the three peaks in *s* PDOS. The observed anisotropy of the L_3 edge is much smaller than that found at the *K* edge, which confirms the *s* character of projected states. However, the similarity of the CB states of *s* and *d* symmetry indicates strong hybridization of these states up to 12 eV. The *d* PDOS obtained from the calculations should produce in the measured spectrum a broad maximum between 13 and 15 eV, but it is not observed, suggesting that the matrix element for $2p$-$4d$ transitions is small. Regarding the $M_{2,3}$ spectra [Fig. 1(d)] one can notice that though the spectral resolution is high (0.04 eV) and the natural width of the $3p$ levels is small, only the first minimum and another one around 17.5 eV are well resolved. This may be due to overlap of the spin-orbit-split bands; however, a close similarity of the measurements with the combined s+d DOS suggests that the $3p$-$4d$ transition rate is comparable with the $3p$-$4s$ transition rate. Comparing Figs. 1(c) and 1(d) we can conclude that the shape of L_3 edge is dominated by *s* conduction states, whereas the shape of $M_{2,3}$ edge by *s* and *d* states. The observed differences in the shape of L_3 and $M_{2,3}$ edges indicate the differences in the transition matrix for $2p$ and $3p$ core levels to $4s$ and $4d$ conduction states.

The results for GaN in the cubic structure are presented in Fig. 2. The general features of calculated PDOS and measured spectra, especially at the N site, are very similar in the cubic and wurtzite cases. Some differences are in the distribution of *s* and *d* states at Ga site—there are decidedly fewer states of Ga *d* symmetry in the cubic structure. However, the general shape of the Ga L_3 edge has the same character as in the wurtzite phase, which confirms that the transition matrix to *d* states is small. Summarizing, the main features of wurtzite and cubic GaN structures are (i) the dominant character of *p* states, particularly at the N site, for both VB and CB, (ii) the dominant contribution of *s* states of Ga at the bottom of the VB

for cubic structure and smaller contribution of these states for wurtzite structure, and (iii) significant hybridization *p*- *d*(Ga) at valence- and conduction-band edges.

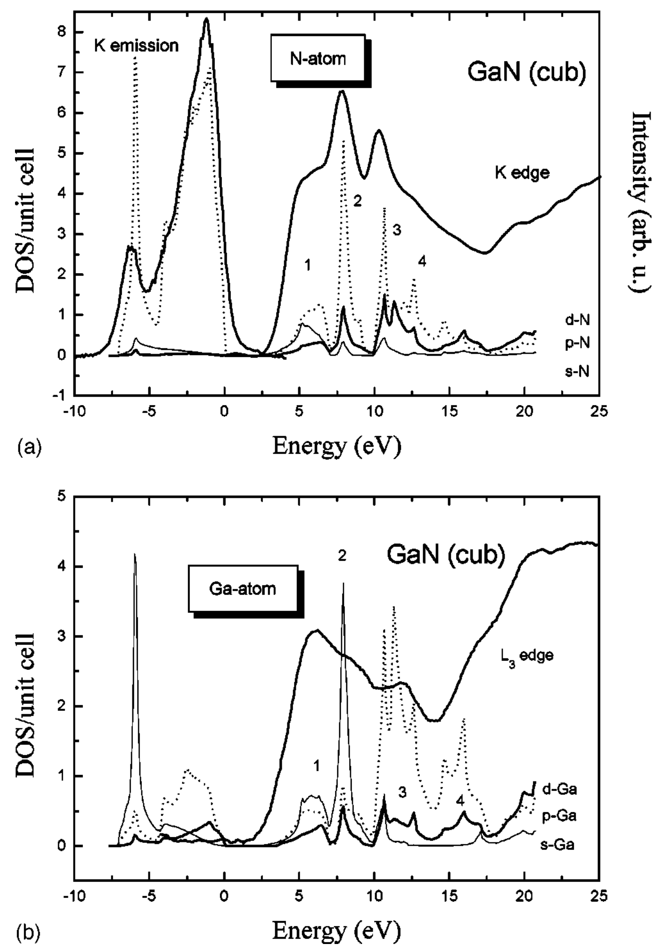

Figure 2 The PDOS (*s* thin line; *p*, dotted line, *d*, thick line) as calculated for the cubic structure of GaN. (a) Projected on the N atom and compared with N *K* emission and absorption spectra. (b) Projected on the Ga atom and compared with the Ga L_3 absorption spectrum.

Although the AlN wurtzite PDOS and the measured x-ray spectra (presented in Fig. 3) are essentially similar to those for GaN, some differences exist. One pronounced difference is that at the AlN CB edge the *d* states of cation dominate over *s* states, contrary to the GaN case. In VB and CB the Al states of *p* as well as *d* symmetry are located at the same energy as the density maximum of N states of *p* symmetry, reflecting the strong hybridization of these states. As it was already mentioned in the Introduction, *p-d* hybridization may be one of the reasons for the much larger energy gap of AlN in comparison with GaN. Considering the higher-energy part of CB (up to 13 eV) there is a smaller amount of *d* states and bigger contribution of *s* states of the cation [Fig. 3(c)], but, as in GaN, the similarity of the states of *s* and *d* symmetry indicates strong hybridization of these states. The second, even more pronounced difference is connected with *u*- and *rr*-bond distribution. In AlN the anisotropy of tion states distribution is very pronounced at the anion as well as at the cation site [Figs. 3(a) and 3(b)]. The second peak in the CB localized at the N atom has a *u*-bond origin, whereas only the states with *rr*-bond character contribute to this peak at Al site. The reported polarization-dependent.

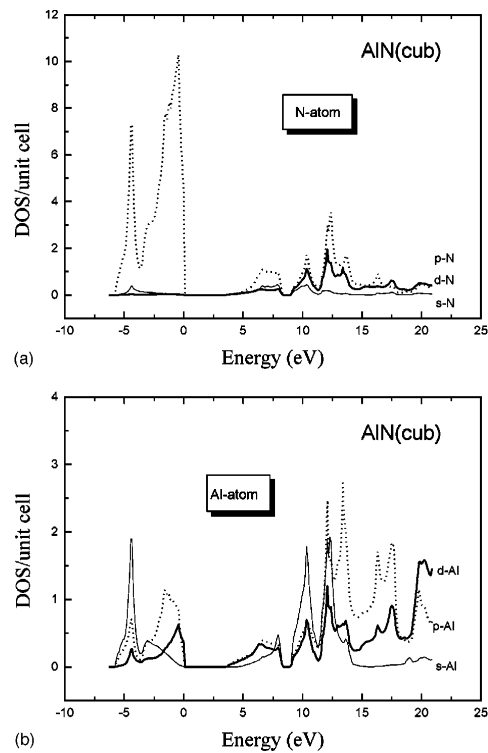

Figure 3 The PDOS (*s* thin line; *p*, dotted line; *d*, thick line) as calculated for the wurtzite structure of AlN. (a) Projected on the N atom and compared with N *K* emission and absorption spectra measured for *rr* and *u* polarization geometry. (b) Projected on the Al atom: *p* PDOS compared with Al *K* absorption spectra measured for *rr* and *u* polarization geometry, additionally the mixed-bond spectrum is shown (dotted line).

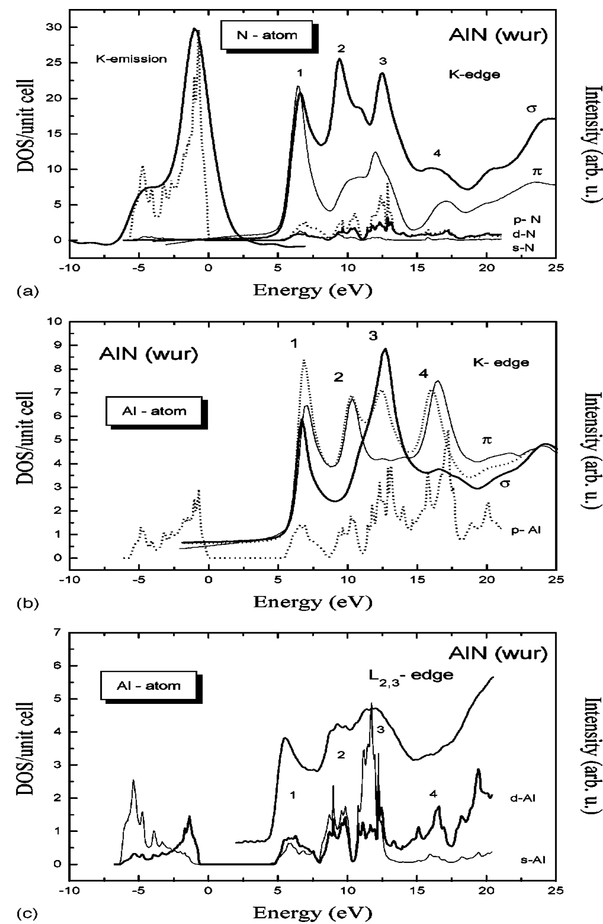

Figure 4 The PDOS (*s*, thin line; *p*, dotted line; *d*, thick line) as calculated for the cubic structure of AlN. (a) Projected on the N atom. (b) Projected on the Al atom.

spectra give clear evidence that the bonds formed in plane and out of plane are different, and as in the case of GaN, this should infuence the transport and optical properties in the two directions. Stronger anisotropy of the distribution of states in AlN seems to be connected with the differencemuch larger than that in GaN between the *u* and *rr* bond lengths. Figure 3(b) also contains the mixed polarization spectrum, which can be compared directly with calculated *p* PDOS. In Fig. 3(c) the Al absorption near the $L_{2,3}$ edge is shown together with Al *s* and *d* PDOS. We donot resolve L_2 and L_3 edges because the L_2 edge is supressed by a Koster-Kronig Auger transition. We did not have access to sufficient-quality samples of cubic AlN, and therefore only the calculated DOS are presented in Figs. 4(a) and 4(b). Generally, the PDOS is similar to the case of wurtzite AlN. The *p* states dominate at the CB edge, as in wurtzite case.

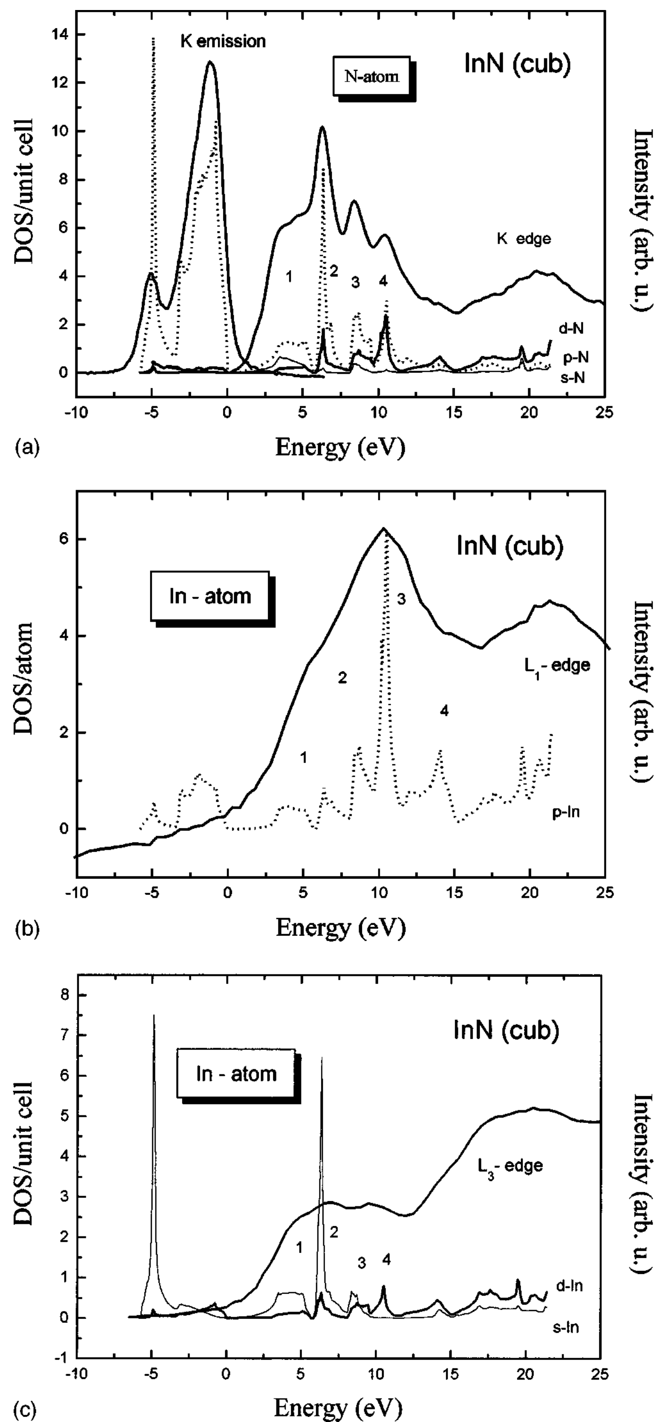

Figure 5 The PDOS (*s*, thin line; *p*, dotted line; *d*, thick line) as calculated for the wurtzite structure of InN. (a) Projected on the N atom and compared with N *K* emission and absorption spectra mea- sured for *rr* and *u* polarization geometry. (b) projected on the In atom: *p* PDOS and L_1 absorption spectra for *rr* and *u* polarization geometry. (c) Projected on the In atom: *s* and *d* PDOS and L_3 absorption spectra for *rr* and *u* polarization geometry.

As one can see from the Fig. 5 the calculated PDOS distribution and experimental spectra for InN resemble those forGaN. In particular, the *p*-PDOS distribution and the general shape of the *K*-edge spectrum at N and at the cation site are very similar. Also, the anisotropy of *rr* and *u* bonds is not so strong as in AlN, but comparable with the GaN case. On the other hand, only in the case of InN do we observe at the CB edge a shift in the binding energy of the *rr* bond with respect to the *u* bond. At the N site this shift is about 0.8 eV [Fig. 5(a)]. A similar effect, although less pronounced, is seen for the *L* edge at In site [Figs. 5(b) and 5(c)]. It suggests an anisotropy of the InN band gap around the r point. In con trast to the situation in GaN, we have more *u* states close to the CB edge. Therefore, in ternary $In_xGa_{1-x}N$ alloys with low In content, the states of InN *u* bonds can form states in the *c* plane with energy located in the GaN energy gap. For the spectra obtained at the L_1 edge of In [Fig. 5(b)] we did not resolve many details because the natural width of In 2*s* level is 5 eV.[26] However, overall agreement of the location of main maximum and minimum compares well with the calculated *p* PDOS distribution. Comparing to GaN, we find only the first and second peaks in PDOS are widely separated while the third and fourth peaks consist now of an assembly of a few other overlapping peaks.

In Fig. 5(c) measurements obtained at the L_3 edge of In together with the *s* and *d* PDOS of In are shown. The In 2 $p_{3/2}$ level has a natural width of 2.65 eV and limits the number of details that can be resolved. The *rr* and *u* bonds are almost equally distributed; only at the third maximum in PDOS does the main contribution come from *u* bonds. Three well-separated peaks in *s* PDOS are especially similar to those observed in GaN. The *d* PDOS distribution is different. There is a considerably smaller contribution of *d* states of cations to CB than in GaN or even AlN.

4. CONCLUSIONS

The large set of the x-ray spectra for group-III nitrides with wurtzite (and BN hexagonal) and cubic structure are presented and discussed together with the ''raw'' PDOS en- ergy distribution calculated using the LMTO method. In the case of GaN, AlN, and InN the agreement between the cal- culated partial density of states distribution and observed spectra is very good. This allows us to perform a detailed analysis of characteristic features of DOS, especially in con- text of partial DOS contributions to total DOS in VB and CB. Moreover, some important conclusions about hybridization of *p-d* and *s-d* states are drawn. General features of the spectra for GaN and InN are very similar, whereas some differences exist when we compare them with AlN. Thus, can be explained by the lack of the cation semicore *d* states in AlN. Comparing the PDOS distribution between the wurtzite and cubic structure of considered compounds we also found close similarities. However, for the cubic structure more states are localized at the bottom of the VB, and in the CB the fourth peak is generally better separated and more visible than in the wurtzite structure.

References

[1] Maria Serneiroda Dunkha, A. Vincent, Exp. Theo. NANOTECHNOLOGY 5 (2021) 153
[2] Alvin Luis, Tadres Mauricio, Exp. Theo. NANOTECHNOLOGY 5 (2021) 157
[3] V.A. Gubanov, Z.W. Lu, B.M. Klein, and C.Y. Fong, Phys. Rev. B 53 (1996) 4377
[4] A. Loiseau, F. Willaime, N. Demoncy, G. Hug, and H. Pascard, Phys. Rev. Lett. 76 (1996) 4737
[5] B. D. Kim, T. Pan. J. G. Kim, Exp. Theo. NANOTECHNOLOGY 5 (2021) 163
[6] T. Detchprohm, K. Hiramatsu, K. Itoh, and I. Akasaki, Jpn. J. Appl. Phys., 31 (1992) L1454
[7] M. Leszczynski, H. Teisseyre, T. Suski, I. Grzegory, M. Bock- owski, J. Jun, S. Porowski, K. Pakula, J.M. Baranowski, C.T. Foxon, and T.S. Cheng, Appl. Phys. Lett. 69 (1996) 73
[8] N.E. Christensen and I. Gorczyca, Phys. Rev. B 50 (1994) 4397
[9] A. Rubio, J.L. Corkill, M.L. Cohen, E.L. Shirley, and S.G. Louie, Phys. Rev. B 48 (1993) 11 810
[10] W.R.L. Lambrecht and B. Segall, J. Rife, W.R. Hunter, and D.K. Wickenden, Phys. Rev. B 51 (1995) 13 516
[11] Yong-Nian Xu and W.Y. Ching, Phys. Rev. B 48 (1993) 4335
[12] G. Martin, S. Strite, A. Botchkarev, A. Agarwal, A. Rockett, H. Morkoc, Appl. Phys. Lett. 65 (1994) 610
[13] G. Le Marie, C. Cière, C. Selvain, Exp. Theo. NANOTECHNOLOGY 5 (2021) 1
[14] W.R.L. Lambrecht, S.N. Rashkeev, B. Segall, K. Lawniczak- Jablonska, T. Suski, E.M. Gullikson, J.H. Underwood, R.C.C. Perera, J.C. Rife, I. Grzegory, S. Porowski, D.K. Wick-enden, Phys. Rev. B 55 (1997) 2612
[15] K. Lawniczak-Jablonska, T. Suski, Z. LilientalWeber, E.M. Gullikson, J.H. Underwood, R.C.C. Perera, and T.J. Drummond, Appl. Phys. Lett. 70 (1997) 2711
[16] L.C. Duda, C.B. Stagarescu, J. Downes, K. Smith, D. Korakakis, T.D. Moustakas, J. Guo, and J. Nordgren, Phys. Rev. B 58 (1998) 1928

© 2022 The Authors. Published by IFIA (https://etnano.com/). This article is an open access article distributed under the terms and conditions of the Creative Commons Attribution license (http://creativecommons.org/licenses/by/4.0/).